

	Laboratori Nazionali di Frascati		
		DIVISIONE TECNICA E DEI SERVIZI GENERALI	
Numero DT <i>DT Number</i>	Data <i>Date</i>	Pagina <i>Page</i>	
DT- MATN-2010-04-01	1 Aprile 2010	1 di 30	
Documento tipo / <i>Document type</i> <p style="text-align: center;">TECHNICAL NOTE (TN)</p>			
Titolo / <i>Title</i> <p style="text-align: center;">The Septum Like Quadrupole for the Super-B Interaction Region (alternative solutions)</p>			
Autori (DT se non diversamente indicato) / <i>Authors (DT if non differently indicated)</i> Claudio Sanelli ¹ ¹ Laboratori Nazionali di Frascati - Via E. Fermi,40 - I-00044 Frascati (Rome) Italy			
Indirizzo per comunicazioni / <i>Contact person</i> Claudio.sanelli@lnf.infn.it			
Parole chiave / <i>Keywords</i> Super-B, Interaction Region, quadrupole, magnets			
Riassunto / <i>Abstract</i> <p>Questa nota tecnica descrive il progetto dei quadrupoli prospicienti il punto di interazione dei fasci della Super-B, nella versione elettromagnetica.</p> <p>The twin quadrupoles near the interaction point (IP) of the Super B, in the electromagnetic version, are described in this technical note.</p>			
Nome file / <i>Filename</i>	Versione / <i>Version</i>	Distribuzione / <i>Distribution</i>	Visibilità / <i>Access</i>
The septum like Quadrupole TecNote.doc	1	DT-DA	DESIGN
Preparato / <i>Compiled</i>	Controllato / <i>Controlled</i>	Controllato / <i>Controlled</i>	Approvato / <i>Approved</i>
Claudio Sanelli	Claudio Sanelli		
1 Aprile 2010	1 Aprile 2010		

	The septum like quadrupole for the Super-B Interaction Region (alternative solutions)	DT Numero / <i>Number</i>	Data / <i>Date</i>	Pagina / <i>Page</i>
		DT-MATN-2010-04-01	1 Aprile 2010	4 di 30

**The Septum like Quadrupole
for
the Super B Interaction Region
(Alternative Solutions)**

INDEX

1. Introduction.....	5
2. Design criteria.....	5
3. Basic geometry.....	6
4. Simulation in 2D – POISSON Code.....	7
5. Quadrupole parameter list.....	12
6. Quadrupole “unbalancing” (20-40%) – 2D Simulations.....	15
7. Simulations in 3D – Opera© Code.....	21
8. Work to do	27
8.1 Simulation refinement.....	27
8.2 Pole profile optimization.....	29
8.3 Coil Terminal optimization.....	29
8.4 Pole chamfer optimization	30
9. Conclusions.....	30

	The septum like quadrupole for the Super-B Interaction Region (alternative solutions)	DT Numero / <i>Number</i>	Data / <i>Date</i>	Pagina / <i>Page</i>
		DT-MATN-2010-04-01	1 Aprile 2010	5 di 30

The Septum like Quadrupole for the Super B Interaction Region (Alternative Solutions)

1. Introduction

Strong focusing quadrupole magnets are needed in the Super B interaction region. The peculiarity of such a quadrupoles is that two quadrupoles have to be located one near the other, upstream and downstream the Interaction Point (IP), and that the field gradient profile, looking from the IP, must be the same in the two quadrupoles.

Many solution have been studied with different kind of structures: pure superconducting quadrupoles (by Paoloni et al.); hybrid superconducting magnets, using Permendur material, to confine the magnetic field (by Vobly).

Since it seems that the use of iron is now accepted, in the following solutions based on this technology are studied. Two possible solution are investigated: they differ on the presence or not of a slab of iron in between the two quadrupoles. The central slab of iron is not necessary in theory, if the quadrupoles are excited by the same current, or if the same gradient is requested. But if we assume, in principle, that the two quadrupoles may have a different exciting currents, or gradients, the central slab will be useful to compensate the magnetic asymmetry. In any case, the presence of this iron slab will made much more mechanically stable the all structure.

The basic main parameters for the design of the magnets are summarized in the following table I.

Integrated Gradient	T	40
Expected maximum Gradient	T/m	100
Total length	m	0.4
Minimum Beam-Beam centre distance	mm	33
Beam pipe external radius	mm	10
X Beam-Beam total crossing angle	mrاد	66

Table I.

2. Design criteria

Due to the lack of available room, solutions with soft iron (ARMCO, US 1010 or 1006) have been adopted, considering that with this kind of irons a good control in the change of the requested field gradient can be obtained. The use of materials with a very sharp

permeability variation is suggested if the working point is practically fixed but it is contraindicated if the regulation range is enough large. This second case has been assumed as a design criterion. Another design criterion comes from the very small space to allocate the excitation coil. Since standard copper holed conductors can not be used, the criterion to have a copper bar of variable cross section with a stainless steel (AISI 316L or similar) tube of special cross section, brazed on the copper bar has been adopted. This technology is the one normally used in the design of septum magnets. The use of the iron allows to shape the iron pole in such a way that the magnetic field harmonic content can be minimized, since the 12-pole component can be cancelled by a proper end pole chamfering. In the following an hyperbolic pole profile has been assumed, schematized by an enough number of straight segments. Electric and hydraulic connections are assumed on the side of the quadrupole far from the IP, meanwhile on the near side the copper/ss tube is simply bent by 180° coming back as return coil. The cooling tube has been assumed having 3*5 mm² external cross section, with 0.25 mm wall thickness for a useful 2.5*4.5=11.25 mm² for demineralized water flow. A thin layer of kapton about 50 µm can be used to isolate the current conducting copper bar from the iron and the other copper bars of the near poles.

3. Basic geometry


Assuming a Cartesian system centered on the beam axis, the upper right iron pole profile is schematized by the points having the coordinates listed in table II.

Point		x (radial)	y (vertical)
A	cm	0.5	1.0
B	cm	0.5261	0.9504
C	cm	0.5797	0.8625
D	cm	0.624	0.801
E	cm	0.707	0.707
F	cm	0.801	0.624
G	cm	0.8625	0.5797
H	cm	0.9504	0.5261
I	cm	1.0	0.5

Table II.

The coordinates of the points of the other quadrupole poles will be symmetric with respect to the Cartesian axes.

The minimum copper bar cross section has been fixed to 3*7.5=22.5 mm². This corresponds to the minimum cross section on the side near the IP, at about 0.5 m from the IP. The maximum copper cross section has been assumed 16.2*7.5=121.5 mm² in the case without the central iron slab and 12*7.5=90 mm² in the case with central iron slab on the side opposite to the IP, at about 0.9 m from the IP. The mechanical length of the quadrupole has been assumed, at this stage, of 0.4 m. This value must be

	The septum like quadrupole for the Super-B Interaction Region (alternative solutions)	DT Numero / <i>Number</i>	Data / <i>Date</i>	Pagina / <i>Page</i>
		DT-MATN-2010-04-01	1 Aprile 2010	7 di 30

decreased by about 1 cm, the bore radius, to fit the requested magnetic length but this will be subject of 3 D calculations.

4. Simulation in 2D – POISSON Code

Simulation in 2D have been performed by means of POISSON, the well known Los Alamos code, version 7.17.

Since the upper halves of the two quadrupoles have been simulated, the Cartesian coordinate system has been centered at the centre of the structure, that means on the bisectrix of the total horizontal 66 mrad beam-beam crossing angle.

The following figure 1 shows the geometry corresponding to the side near the IP; figure 2 shows the magnetic field profile on the horizontal axis and figure 3 shows the gradient (dBy/dx) on the same axis. Figure 4 is a zoom of figure 3 in the area near the centers of the beams. The distance between the centers, of the beams at 0.5 m from the IP, is 33 mm. The value of the gradient is larger than 100 T/m.

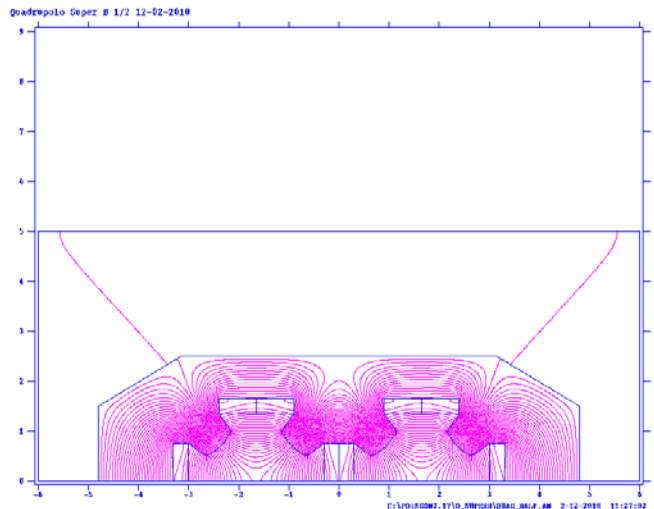


Figure 1: Geometry of the two quadrupoles, side near the IP.

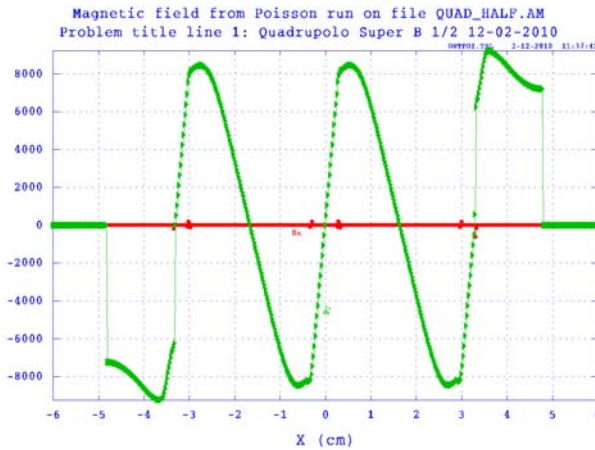


Figure 2: Magnetic field profile along x axis.

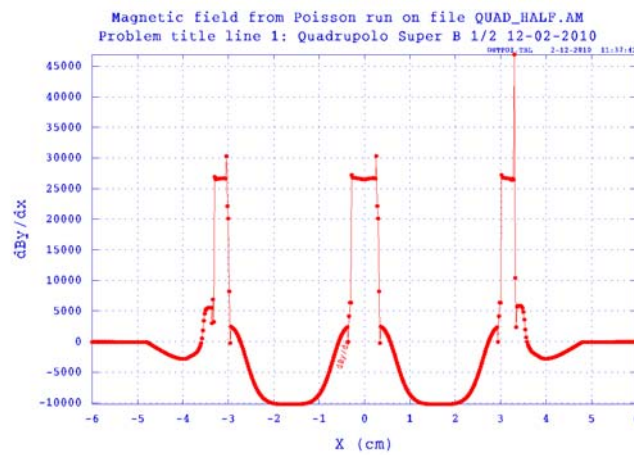


Figure 3: Gradient dB_y/dx along the x axis.

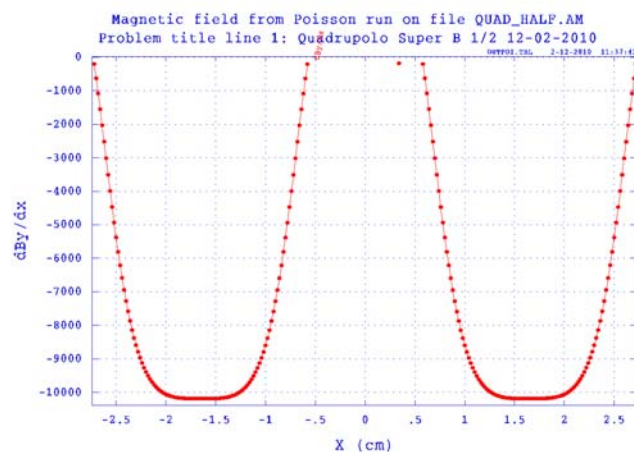


Figure 4: Zoom of figure 3. The position of the beams corresponds to -1.65 and +1.65 cm.

In the following, figure 5 shows the geometry corresponding to the far side from the IP, at 0.9 m from the IP, in the case without central iron slab; figure 6 shows the magnetic field profile on the horizontal axis and figure 7 shows the gradient profile (dB_y/dx) on the same axis. Figure 8 is a zoom of figure 7 in the area near the centers of the beams.

The distance between the centers of the beams is 59.4 mm at this location. The value of the gradient is still larger than 100 T/m and has the same value that in the previous case, about 101.7 T/m.

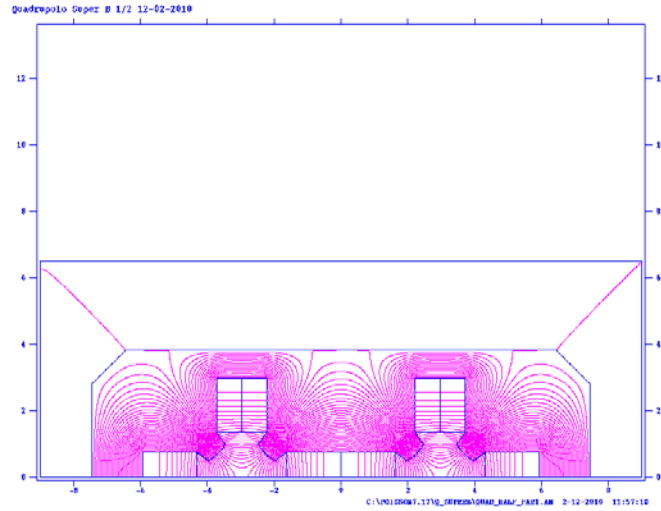


Figure 5: Geometry of the two quadrupoles, side far from the IP.

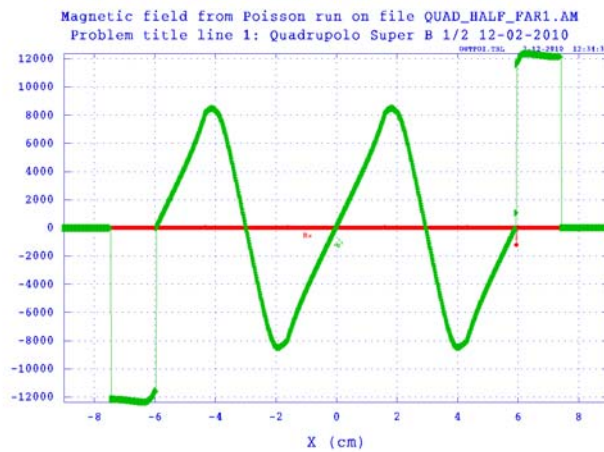


Figure 6: Magnetic field profile along x axis. Side far from the IP.

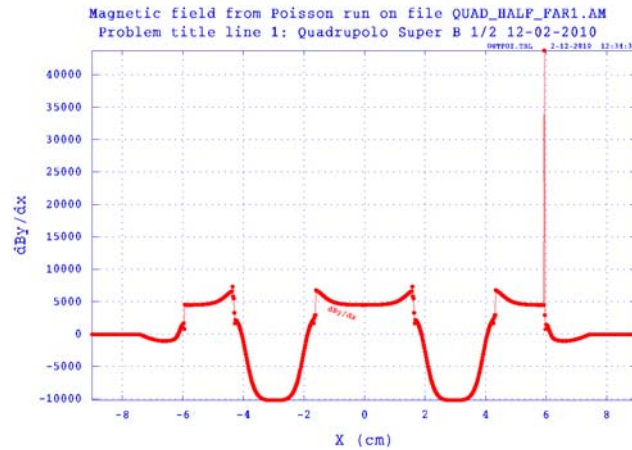


Figure 7: Gradient $\frac{dB_y}{dx}$ along the x axis. Side far from the IP.

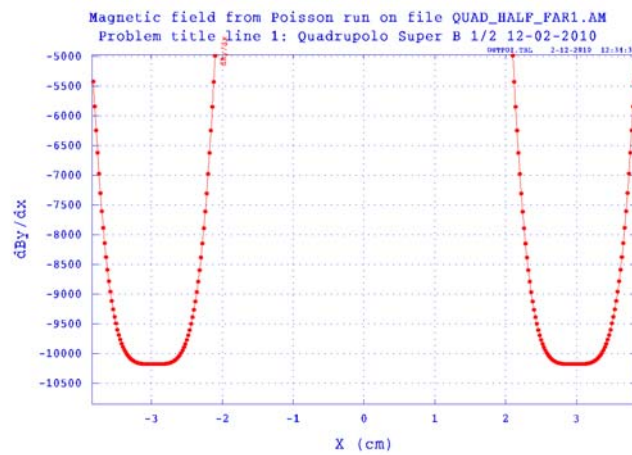


Figure 8: Zoom of figure 7. The distance between the centers of the beams is 5.94 cm.

In the following, figure 9 shows the geometry corresponding to the far side from the IP, in the case with the central iron slab; figure 10 shows the magnetic field profile on the horizontal axis and figure 11 shows the gradient profile ($\frac{dB_y}{dx}$) on the same axis. A zoom of figure 11 is shown in figure 12. The distance between the centers of the beams is maintained be 59.4 mm. The geometry of the side near the IP is the same in both two cases, with and without central slab.

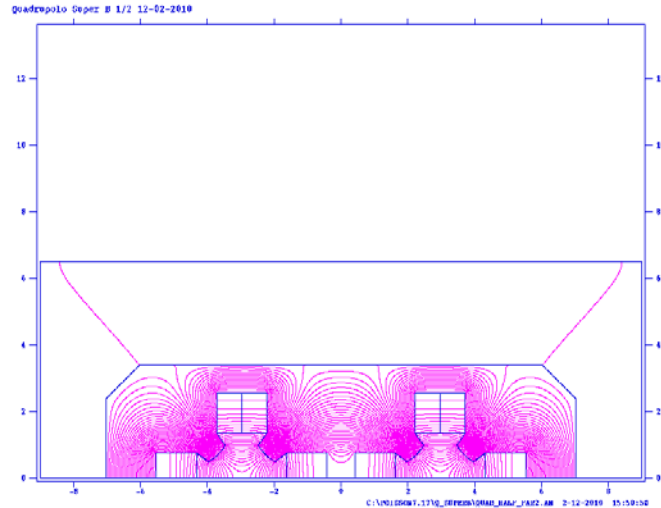


Figure 9: Geometry of the two quadrupoles, side far from the IP. Case with an iron slab in between.

As expected, the central iron slab is not affected by the magnetic flux since the condition of full symmetry is respected. The excitation current needed for about 100 T/m has been found to be 4300 A. All cases shown relate to this current value.

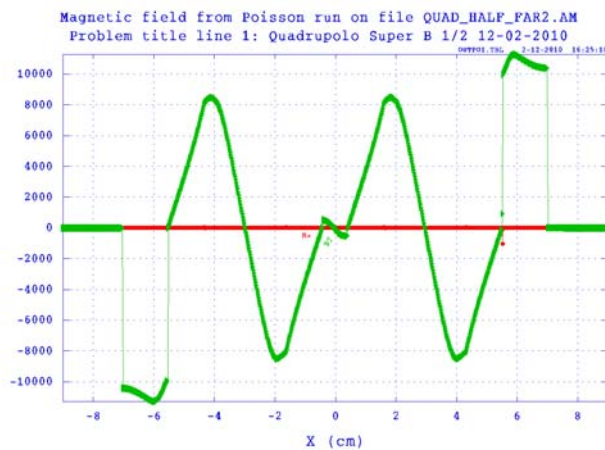


Figure 10: Magnetic field profile along x axis. Side far from the IP. Case with central iron slab.

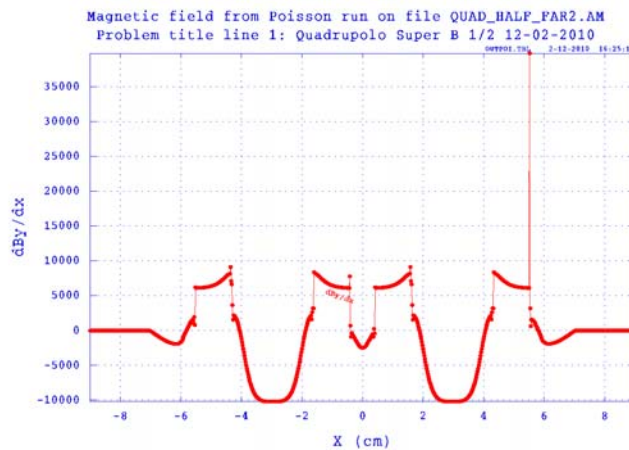


Figure 11: Gradient dB_y/dx along the x axis. Side far from the IP. Case with a central iron slab.

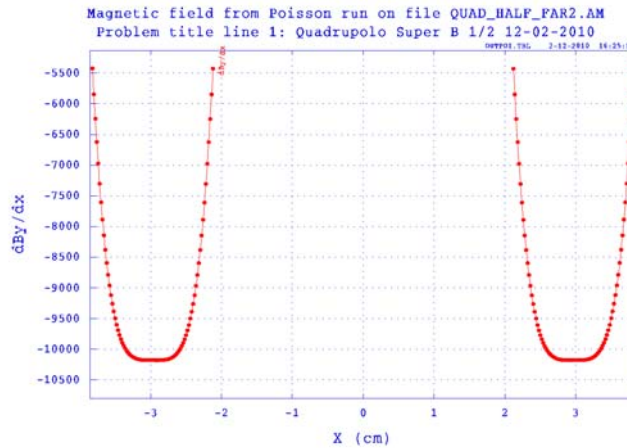


Figure 12: Zoom of figure 11. The distance between the centers of the beams is 5.94 cm. Case with a central iron slab.

5. Quadrupole parameter list

The simulations made till now have assumed a complete symmetry in the two quadrupoles. The only parameter changed is the cross section of the current carrying copper bar, that is decreasing starting from the far side, with respect to the IP, toward the side near the IP. The assumption is a variation from 121.5 to 22.5 mm² in the case without central iron slab and from 90 to 22.5 mm² in the case with the central iron slab. Also the iron geometry is slightly different. The central iron slab has a thickness of 8.4 mm. Its effect will be considered in the next chapter where the “unbalancing” between the two quadrupoles will be studied.

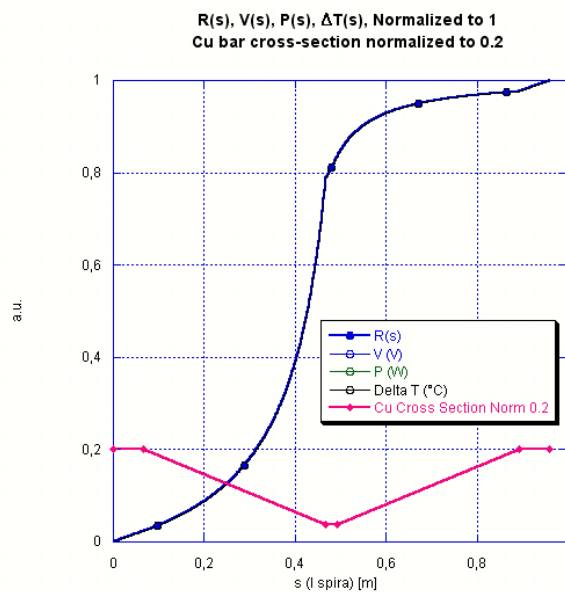


Figure 13: Resistance, Voltage, Power and Temperature increase along the "excitation turn", normalized values.

Figure 13 shows, in the case without the central iron slab, how the resistance of the copper bar changes along the length of the excitation turn, due to the copper cross section variation. The turn length has been assumed be 0.96 m. The excitation current has been fixed to 4300 A. Accordingly, also the voltage, the power and temperature increase change with the same law. What has been assumed constant is the cooling flow of the demineralized water. The table III summarized the main parameters in this first case. The numbers refer to each single quadrupole.

Maximum Gradient	T/m	101.7	
Integrated Gradient	T	40	
Magnetic Length	m	0.4	
Pole Tip Field	T	1	
Magnet Bore Radius	m	0.01	
Turns per pole		1	
Current	A	4300	
Current Density	A/mm ²	35.39	191.11
Copper conductor	mm*mm	7.5*16.2	7.5*3
Copper Area	mm ²	121.5	22.5
Cooling duct (external)	mm*mm	3*5	
Cooling duct (internal)	mm*mm	2.5*4.5	
Resistance (1 turn)	mΩ	0.466	
Magnet Resistance (@ 60°C)	mΩ	1.864	
Voltage per Magnet	V	8.01	
Power (1 turn)	W	8616.1	
Power per Magnet	W	34464.4	
Water circuits per magnet		4	
Water flow per circuit	m ³ /s	1.51E-4	
Total Water Flow	m ³ /s	6.04E-4	
Pressure Drop	MPa	0.5	
Water velocity	m/s	13.4	
Water Temperature Increase	°C	13.7	

Table III.

Referring to table III, particular attention must be put to the water velocity that is very high. This may create vibration especially where the cooling duct change direction, particularly at the end of the quadrupole near the IP, where it is 180° bent to come back, and where the electric and hydraulic connections have to be made.

In the second case, the one with the central iron slab, the change law of the resistance, voltage, power and temperature is a little different from the first one. Figure 14 shows the normalized shape and table IV lists the main parameters in this second case.

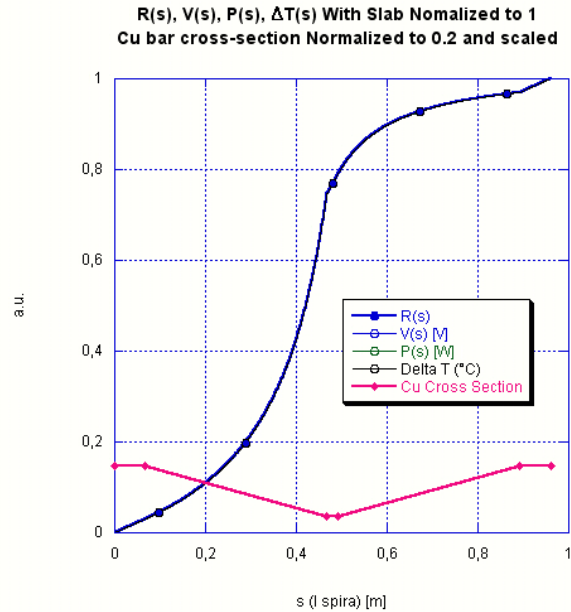


Figure 14: Resistance, Voltage, Power and Temperature increase along the "excitation turn", normalized values. Case with central iron slab.

Maximum Gradient	T/m	101.7	
Integrated Gradient	T	40	
Magnetic Length	m	0.4	
Pole Tip Field	T	1	
Magnet Bore Radius	m	0.01	
Turns per pole		1	
Current	A	4300	
Current Density	A/mm ²	47.77	191.11
Copper conductor	mm*mm	7.5*12	7.5*3
Copper Area	mm ²	90	22.5
Cooling duct (external)	mm*mm	3*5	
Cooling duct (internal)	mm*mm	2.5*4.5	
Resistance (1 turn)	mΩ	0.5	
Magnet Resistance (@ 60°C)	mΩ	1.99	
Voltage per Magnet	V	8.55	
Power (1 turn)	W	9185.8	

Power per Magnet	W	36743.2	
Water circuits per magnet		4	
Water flow per circuit	m ³ /s	1.51E-4	
Total Water Flow	m ³ /s	6.04E-4	
Pressure Drop	MPa	0.5	
Water velocity	m/s	13.4	
Water Temperature Increase	°C	14.6	

Table IV.

6. Quadrupole “unbalancing” (20-40%) – 2D Simulations

To understand the effect of a possible “unbalancing” between the two adjacent quadrupoles, two cases have been simulated: in the first one the current in one magnet has been reduced to the 80% and in the second one to 60% of the nominal 4300 A.

Figure 15 shows the geometry and the magnetic flux line distribution, in the side near the IP, with the right quadrupole having only 60 % of the excitation current of the left one. Figures 16 and 17 show the magnetic field profile in the two cases (80% and 60%) and figures 18 and 19 show the gradient dBy/dx on the horizontal plane.

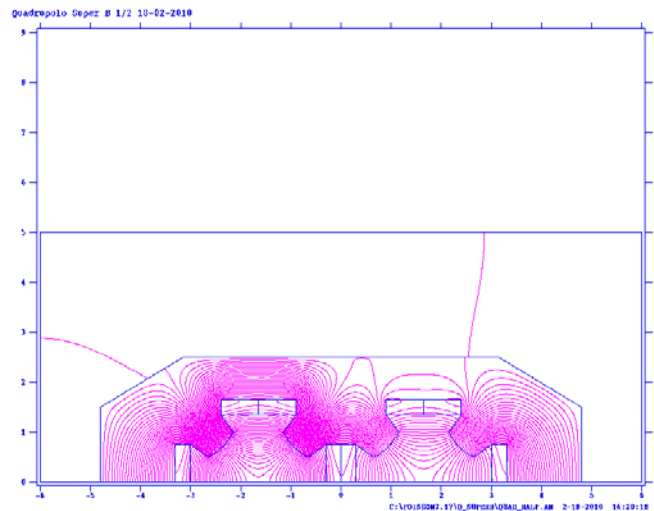


Figure 15: Geometry and magnetic flux distribution with the right quadrupole current at 60%. Side near the IP.

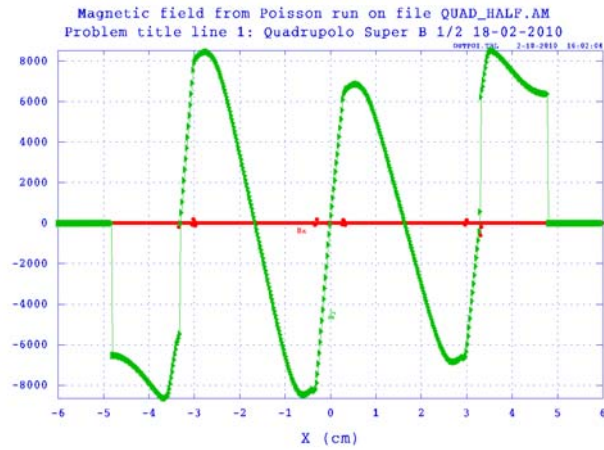


Figure 16: Magnetic field along the horizontal axis with the right quadrupole current decreased to 80%. Side near the IP.

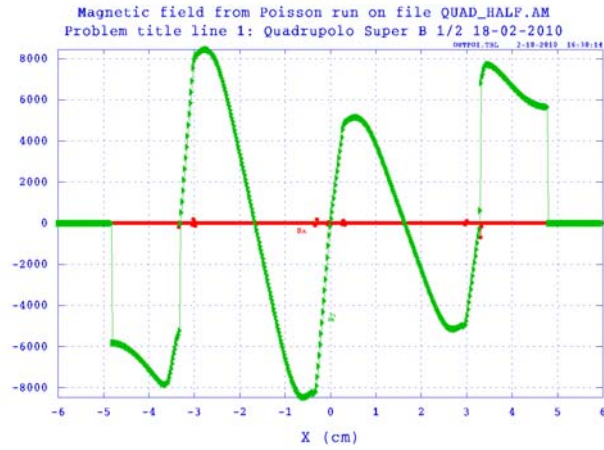


Figure 17: Magnetic field along the horizontal axis with the right quadrupole current decreased to 60%. Side near the IP.

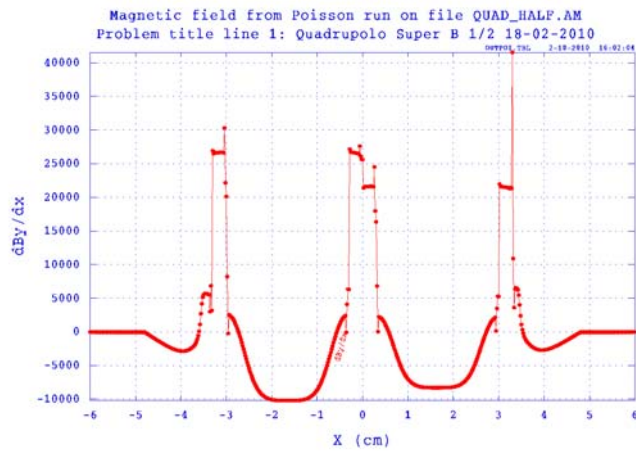



Figure 18: Gradient dB_x/dx along the horizontal axis with the right quadrupole current decreased to 80%. Side near the IP.

	The septum like quadrupole for the Super-B Interaction Region (alternative solutions)	DT Numero / Number	Data / Date	Pagina / Page
		DT-MATN-2010-04-01	1 Aprile 2010	17 di 30

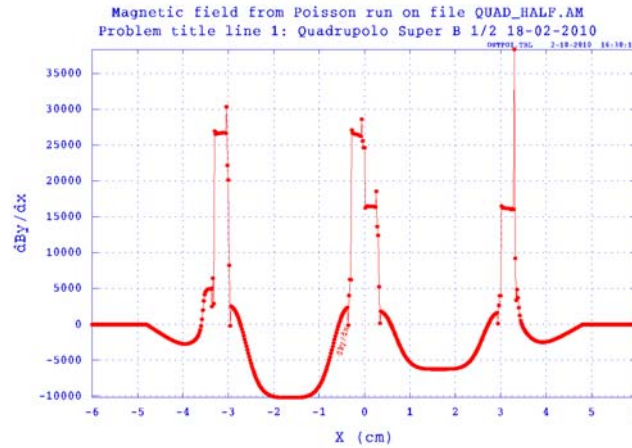


Figure 19: dBy/dx along the horizontal axis with the right quadrupole current decreased to 60%. Side near the IP.

In the first case, with current decreased to 80% (3440 A), the gradient of the left quadrupole is about 100.56 T/m and the gradient of the right quadrupole is about 81.66 T/m. In the second case, current decreased to 60 % (2580 A), the gradient of the left quadrupole is about 100.55 T/m and the one for the right quadrupole is about 61.43 T/m.

The same exercise has been done for the side far from the IP. Figure 20 shows the geometry and the magnetic flux line distribution, in the case of 60% current reduction on the right quadrupole, sub-case without any iron slab in between the two quadrupoles. Figures 21 and 22 show the magnetic field profile on the horizontal axis, respectively in the 80% and 60% current reduction in the right quadrupole. Figures 23 and 24 show the gradient dBy/dx profile, always on the horizontal axis, in the same configuration. The distance between the centers of the beam axes is 5.94 cm.

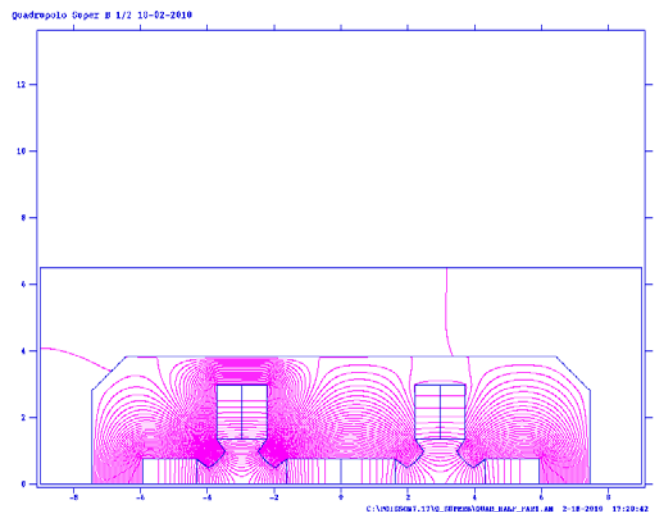


Figure 20: Magnetic field profile on the horizontal axis. 60% current in the right quadrupole. No slab. Side far from the IP.

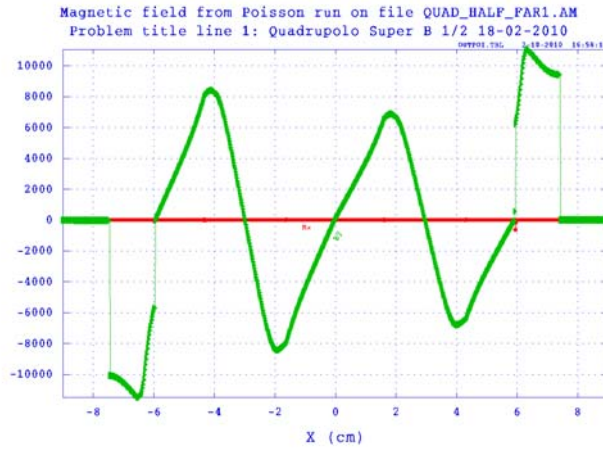


Figure 21: Magnetic field profile on the horizontal axis. 80% current in the right quadrupole. No slab. Side far from the IP.

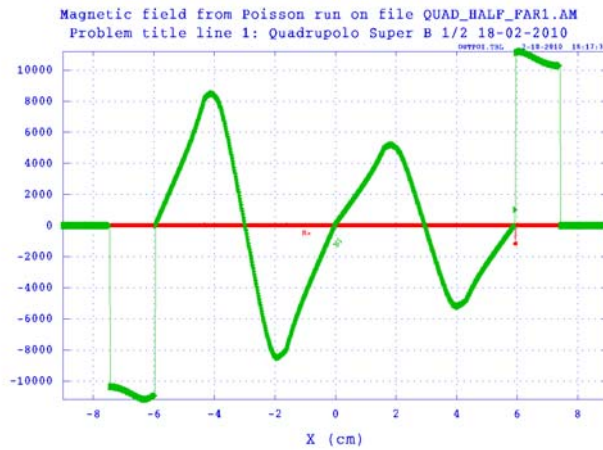


Figure 22: Magnetic field profile on the horizontal axis. 60% current in the right quadrupole. No slab. Side far from the IP.

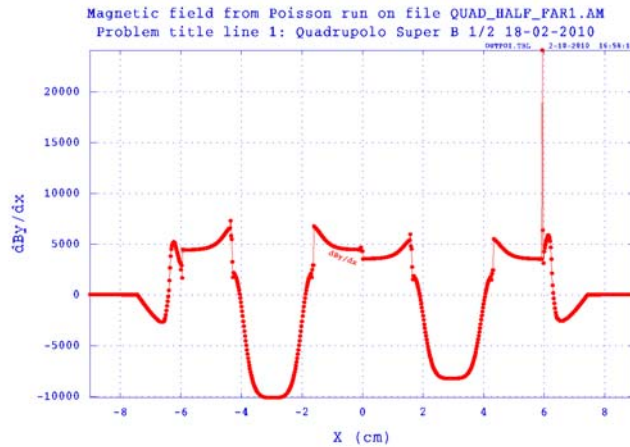


Figure 23: Gradient $\frac{dB_y}{dx}$ profile on the horizontal axis. 80% current in the right quadrupole. No slab. Side far from the IP.

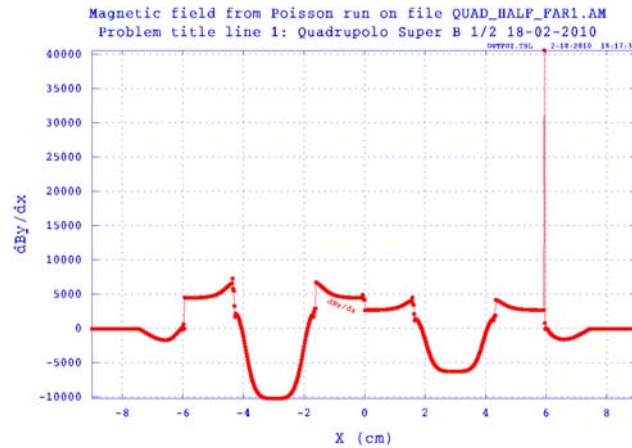


Figure 24: Gradient dBy/dx profile on the horizontal axis. 60% current in the right quadrupole. No slab. Side far from the IP.

The gradient obtained reducing the current to 80% in the right quadrupole is about 99.83 T/m in the left quadrupole and about 81.1 T/m in right one. Meanwhile, reducing the current to 60% the gradient in the left quadrupole is about 100.49 T/m and in the right is about 61.5 T/m.

In the following, the geometry with a central slab of iron has been simulated. Figure 25 shows this geometry at the far side from the IP and the magnetic flux distribution with the current of the right quadrupole decreased to 60%. It must be reminded that the central slab, due to the 66 mrad crossing angle between the two beams, is decreasing its width toward the IP. This effect will better understood with the 3D simulations. It is evident from figure 25 that the central slab help to compensate the asymmetry between the two quadrupoles and that some magnetic flux flows through the iron. Figures 26 and 27 show the magnetic field profile on the horizontal axis respectively in the case of 20 % and 40 % exciting current reduction in the right quadrupole. Again, figures 28 and 29 show the gradient dBy/dx profile on the horizontal axis in the same configuration.

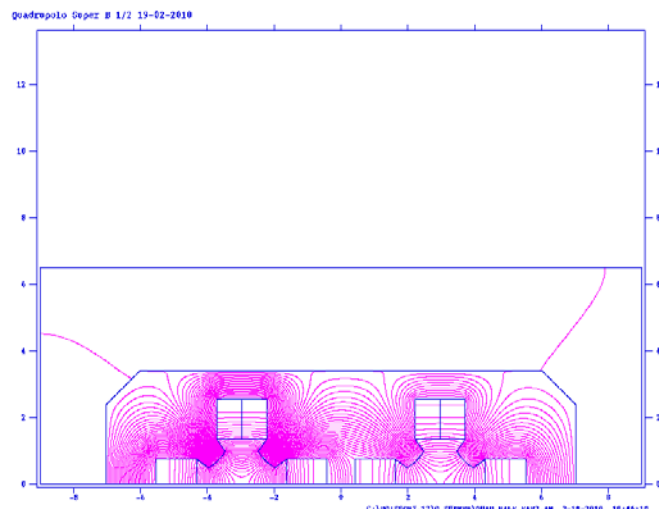


Figure 25: Magnetic field profile on the horizontal axis. 60% current in the right quadrupole. With central slab. Side far from the IP.

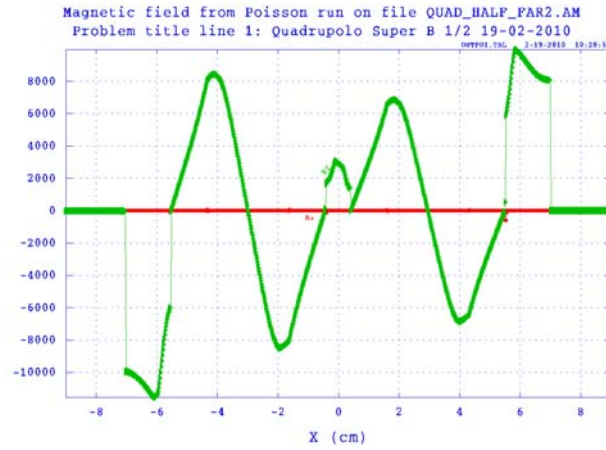


Figure 26: Magnetic field profile on the horizontal axis. 80% current in the right quadrupole. With central slab. Side far from the IP.

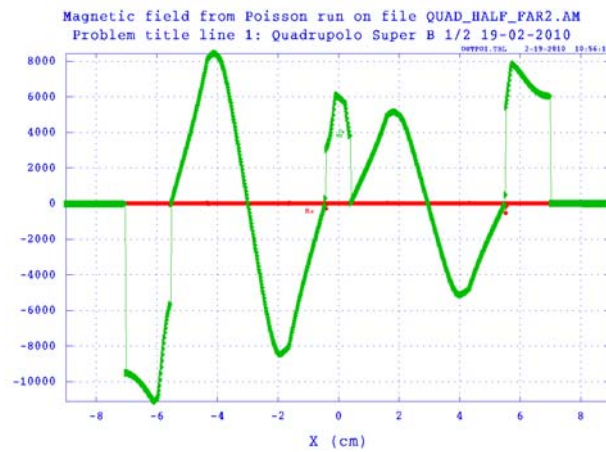


Figure 27: Magnetic field profile on the horizontal axis. 60% current in the right quadrupole. With central slab. Side far from the IP.

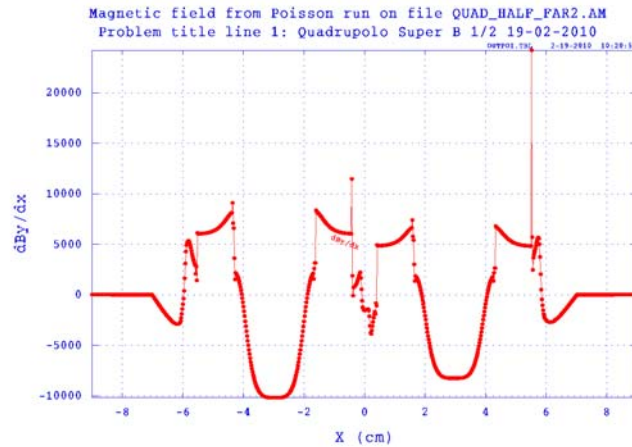


Figure 28: Gradient dB_y/dx profile on the horizontal axis. 80% current in the right quadrupole. With central slab. Side far from the IP.

	The septum like quadrupole for the Super-B Interaction Region (alternative solutions)	DT Numero / Number	Data / Date	Pagina / Page
		DT-MATN-2010-04-01	1 Aprile 2010	21 di 30

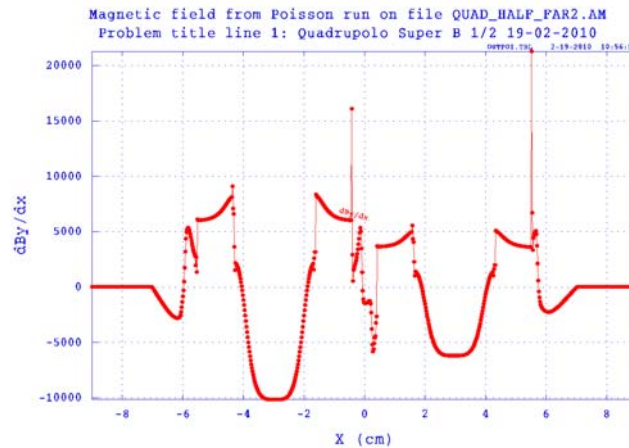


Figure 29: Gradient $\text{d}B_y/\text{d}x$ profile on the horizontal axis. 60% current in the right quadrupole. With central slab. Side far from the IP.

The predicted gradient values, in the case of current reduction to 80% (3440 A) on the right quadrupole are about 100.02 T/m for the left quadrupole and about 81.92 T/m for the right one. The corresponding values in the case of current reduction to 60% (2580 A) are about 100.12 T/m for the left quadrupole and 60.95 T/m for the right one. As it can be seen in figure 27 the magnetic field in this iron cross-section gets an average value of about 0.5 Tesla.

Having in mind that a possible asymmetry may occur for wanted or unwanted reason and considering the parameter lists given in chapter 5, the 3D simulations will be done considering the geometry with the central iron slab.

7. Simulations in 3D – Opera[®] Code

The proposed geometry has been simulated by means of the code Opera[®] Version 13.0. The simulation has been made by simulating only $\frac{1}{4}$ of the full geometry but setting the appropriate symmetries on the y-z and x-z planes. The 3D simulation basically confirm the 2D results and dimensioning. Figure 30 shows the full geometry, from the side far from the IP, the x axis is the radial coordinate, meanwhile the z axis corresponds to the longitudinal one, starting at the IP. The red bars schematize the coil terminals. Figure 31 shows the side near the IP. The water cooling duct is not shown in the figures. It is brazed on the copper conductor and is located between the conductor and the vacuum chamber as described in chapter 2. The mechanical length of the iron yoke has been assumed 0.4 m. The iron starts at 0.5 m and terminates at 0.9 m from the IP. All other parameters are as per table I. For simplicity the iron pole profile has been assumed circular instead of hyperbolic, but the circumference fits the three points A, E and I in table II. The differences on the other points of the pole profile are very small. The excitation current has been set at 4300 A, as per table IV.

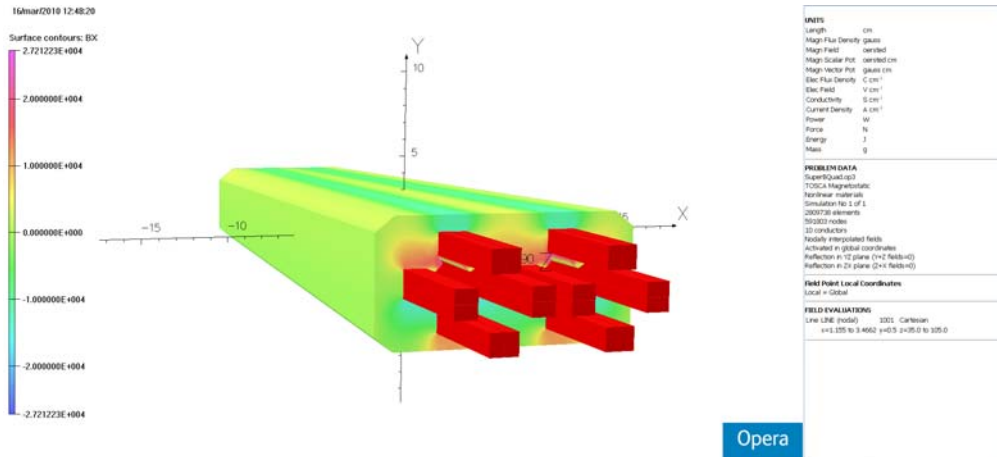


Figure 30: Full Quad geometry. IP far end side.

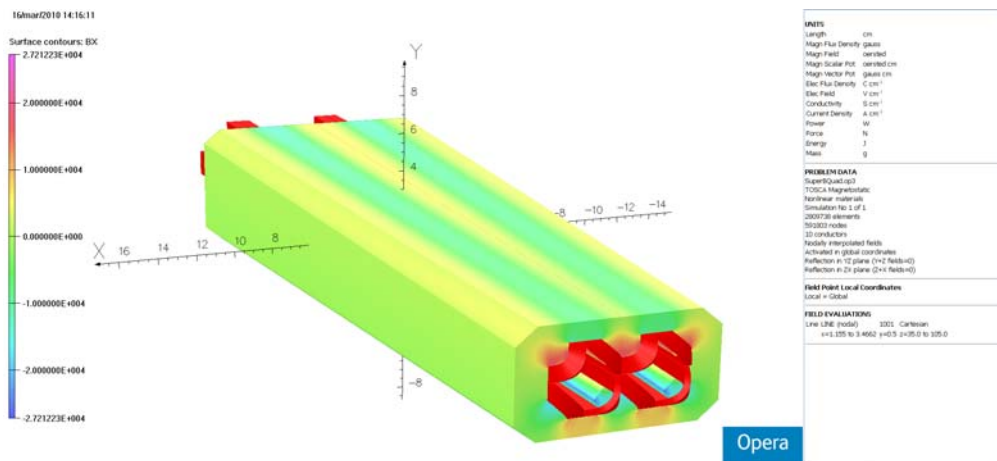


Figure 31: Full Quad geometry. Side near the IP.

Figure 32 and 33 show, respectively, the magnetic flux path on the surface far from the IP and near the IP. The coils have been removed for clarity. Figure 34 shows the BH curve of the iron adopted in the simulation. The Opera© Tenten.bh datafile is equivalent to the US1010 soft iron. Figure 35 shows the “septum like” coil, the water cooling duct is not shown.

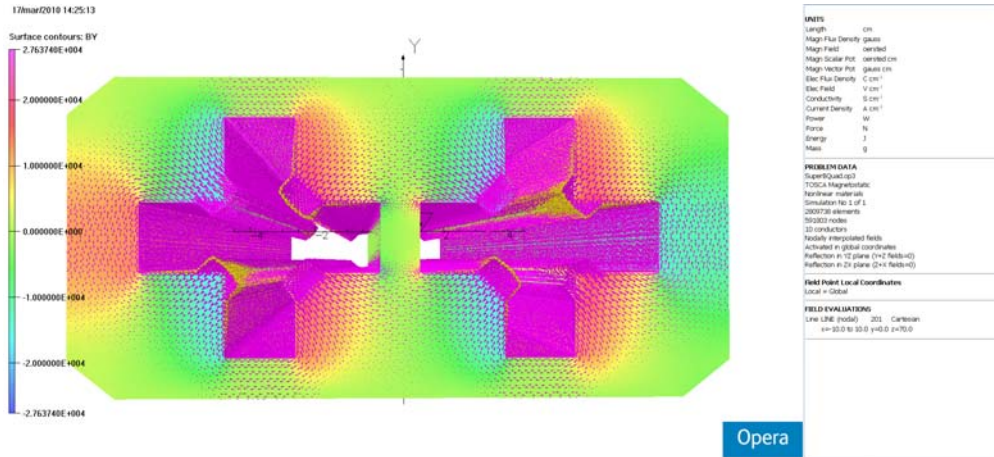


Figure 32: Magnetic flux path on the side far from the IP.

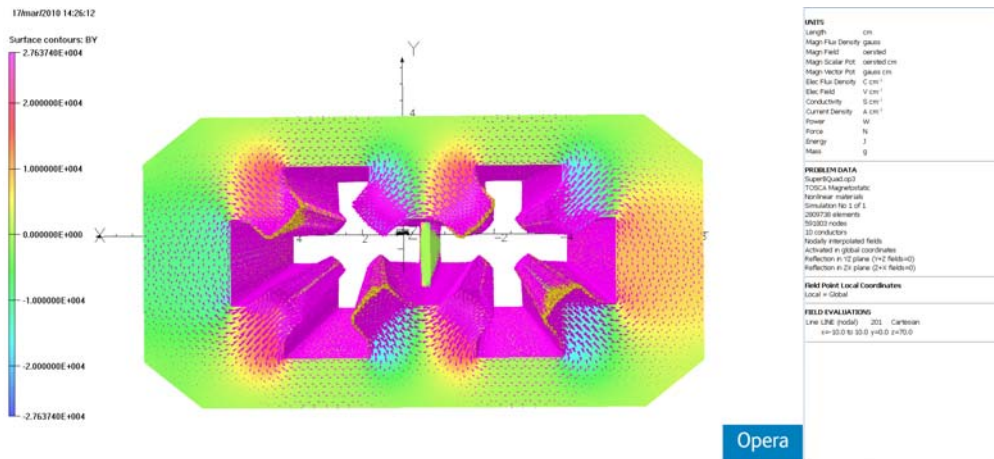


Figure 33: Magnetic flux path on the sead near the IP.

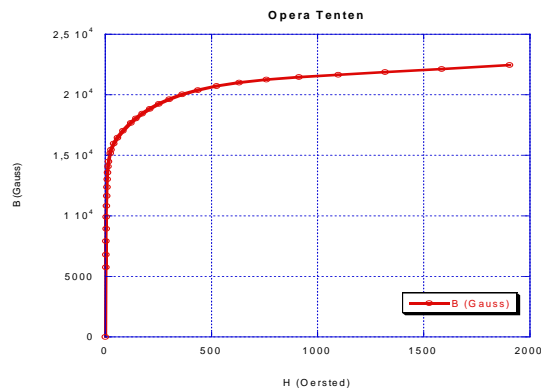


Figure 34: BH curve of Opera Tenten equivalent to US1010 soft iron.

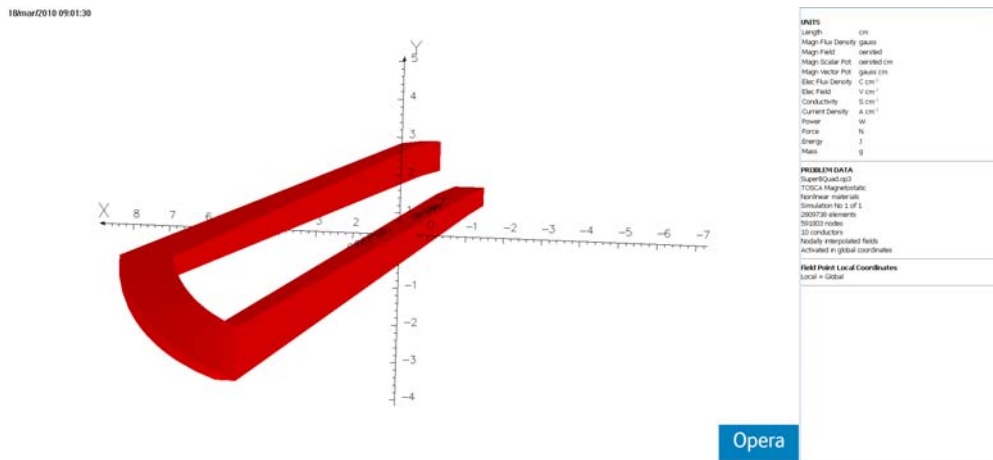


Figure 35: The "septum like" coil.

Figure 36 shows the magnetic field profile at the side near the IP calculated by Opera[®], the x coordinate is the radial coordinate. This picture is equivalent to figure 2, obtained with Poisson. Comparing the two figures one can note that the field peak in figure 36 is lower than in figure 2, due the edge end effect. Figure 37 is the equivalent of figure 10, again the edge end effect is evident.

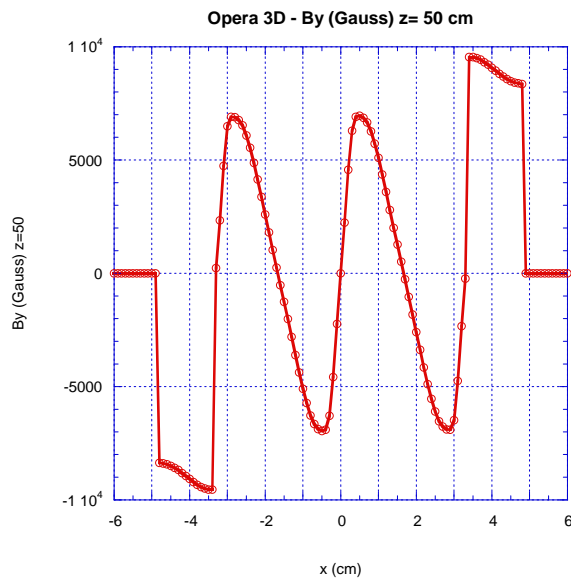


Figure 36: Opera 3D - Magnetic field profile, side near the IP.

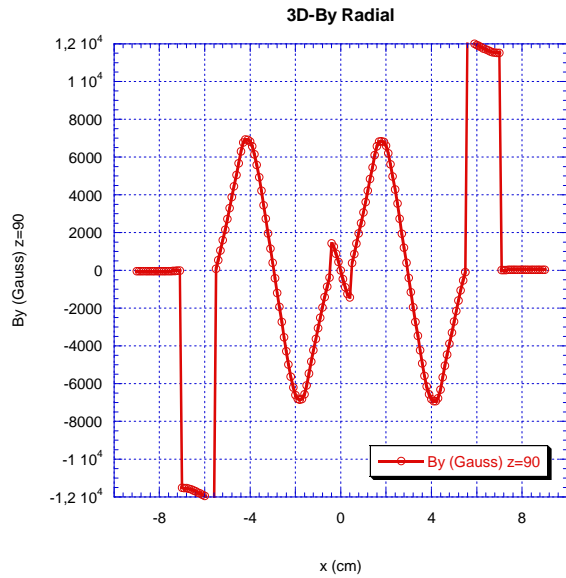


Figure 37: Opera 3D - Magnetic field profile, side far from IP.

Figure 38 is a summary of the radial magnetic field profiles at various longitudinal positions, every 10 cm of iron along the longitudinal coordinate. The zero corresponds to the beam position at the IP.

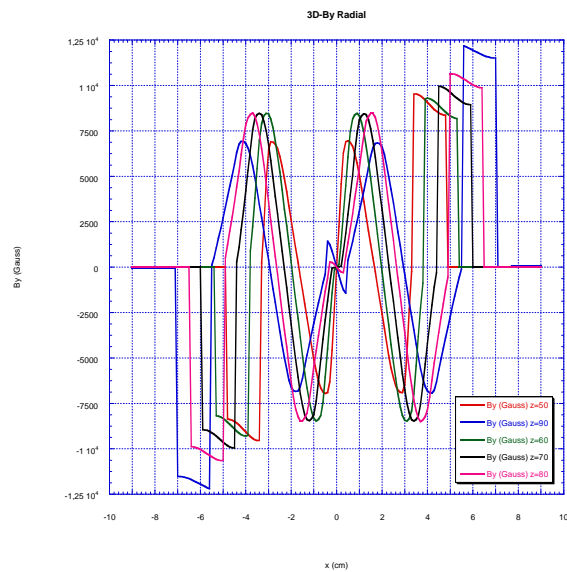


Figure 38: Radial magnetic field profile at various z positions.

Figure 39 shows the gradient profile in the radial direction at the center of the quadrupoles, corresponding to $z=70$ cm from the IP, in Tesla/m. The data are not

interpolated then the mesh discretization is visible. In any case this plot confirm that the gradient of 100 T/m is reached. Figure 40 shows the magnetic field profile along an axis parallel to the beam axis but shifted by 5 mm on the horizontal plane. The magnetic field is greater than 5000 Gauss that at 5 mm from the beam axis corresponds to more than 100T/m. In this figure is clearly visible a field bump at $z > 90$ cm. This is due to the fact that in the simulation a straight bar of length about 6.7 cm has been added at each coil end to allow for terminal interconnections. See figure 30 and 35 for details. Figure 41 is the same of figure 40 but scaled to show the Gradient (T/m) along the same axis, parallel to the beam axis, but shifted by + 5 mm in the x direction. The integral of the curve in figure 41 is about 42.1 Tesla, that is consistent with the fact that the mechanical length of the quadrupole has been assumed of 40 cm and the bore radius is 1 cm. The obtained integrated gradient is in agreement with the desired one, the one listed in table I.

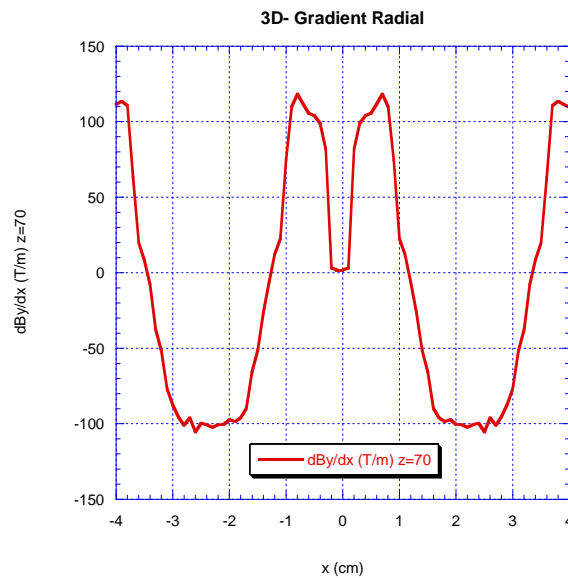


Figure 39: Gradient profile at the quadrupole center along the radial direction.

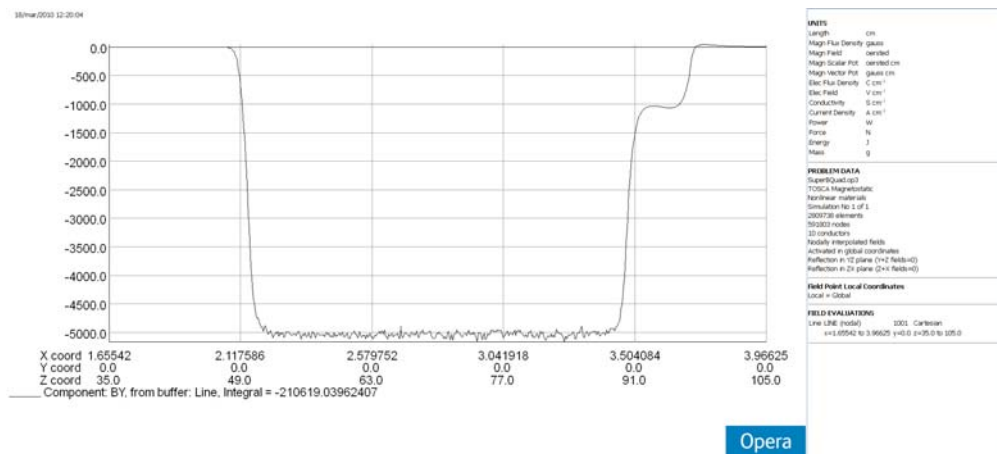



Figure 40: Magnetic field profile along an axis shifted by 5 mm from the beam axis.

	The septum like quadrupole for the Super-B Interaction Region (alternative solutions)	DT Numero / Number	Data / Date	Pagina / Page
		DT-MATN-2010-04-01	1 Aprile 2010	27 di 30

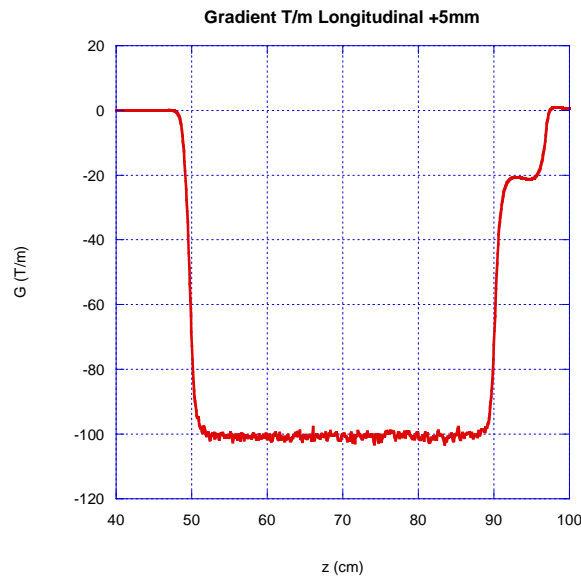


Figure 41: The Gradient (T/m) along an axis parallel to the beam axis, shifted by +5 mm.

8. Work to do

The simulation made till now have demonstrated the feasibility of such alternative solution, in the sense that a twin pair of quadrupoles having the characteristics requested in table I can be built adopting a standard technology. However some more work should be done for a complete and detailed analysis. A not exhaustive list of arguments are pointed out in the following.

8.1 Simulation refinement

Additional work can be done in refining the calculations. Just as an example, figure 42 shows the cross-section of the geometry of the twin quadrupoles seen from side far from the IP, where even the cooling ducts have been added and also the cylindrical vacuum chambers have been drawn. Since the cooling ducts are brazed to the copper bar, a fraction of the current will flow through the duct walls, according the stainless steel tube resistance. Assuming the resistivity of the iron of about $80 \mu\Omega \cdot \text{cm}$ (at 60°C), for a duct length of 0.96 m per coil, one obtains a total resistance of 81.9 m Ω , to be compared to 1.99 m Ω of the copper coils, for each quadrupole. The two resistances are in parallel, then the current flowing in the two circuits can be calculated. Maintaining the nominal value of 4300 A, it can be easily calculated that 4198 A will flow in the copper bar and 102 A in the walls of the cooling ducts. This situation has been simulated (2D simulation) only for the said configuration and the figures 43, 44, 45 and 46 show the results. These figures can be compared with figures 9, 10, 11 and 12,

where the current is flowing only in the copper bar. The comparison shows that the gradient rise down and rise up are sharper in this case than in the previous one.

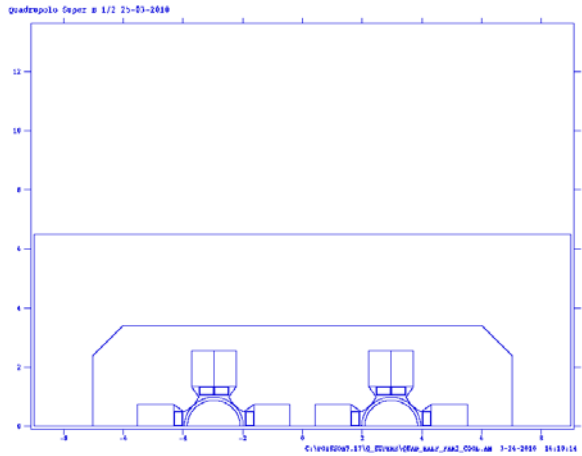


Figure 42: Geometry of the side far from the IP. Cooling ducts and vacuum chambers are also shown.

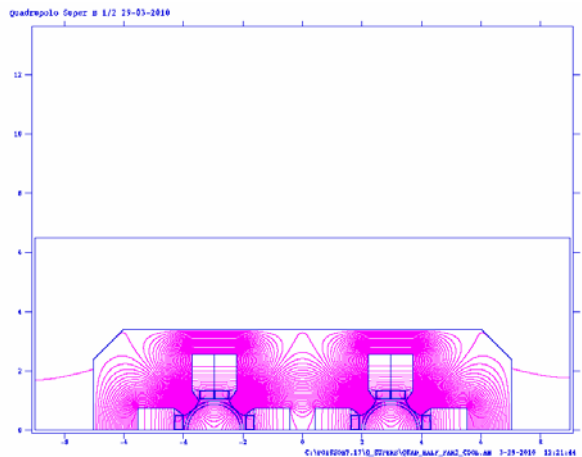


Figure 43: Magnetic flux paths in the case of figure 42.

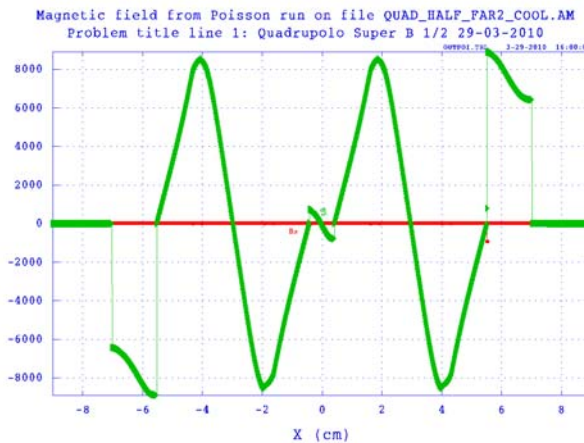


Figure 44: Magnetic field profile along x axis. Same case of figure 43.

	The septum like quadrupole for the Super-B Interaction Region (alternative solutions)	DT Numero / Number	Data / Date	Pagina / Page
		DT-MATN-2010-04-01	1 Aprile 2010	29 di 30

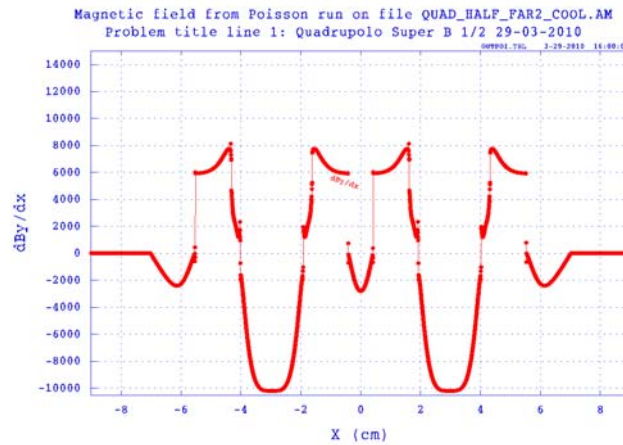


Figure 45: Gradient dBy/dx along the x axis. Same case of figure 43.

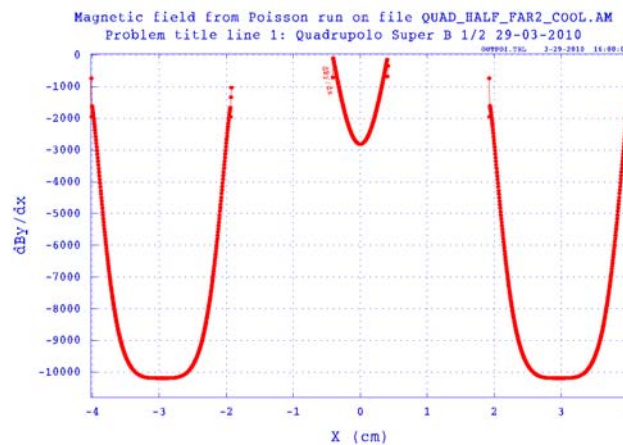



Figure 46: Zoom of figure 45. The distance between the centers of the beams is 5.94 cm.

8.2 Pole profile optimization

The pole profile has been assumed, for simplicity, hyperbolic in the 2D simulations and an arc of circumference in the 3D simulation, fitting the initial, final and central points of the hyperbola, see paragraphs 3 and 7. No harmonic analysis has been accomplished since the study is aimed at to demonstrate that such a kind of structure can be obtained also with a standard technology. A more detailed study to optimize the pole profile should be done if effectively this solution will be considered.

8.3 Coil Terminal optimization

The coil terminals have been assumed as straight bars, see paragraph 7 and figure 30. The effect of these straight bars is evident in figures 40 and 41, where a bump is present

	The septum like quadrupole for the Super-B Interaction Region (alternative solutions)	DT Numero / <i>Number</i>	Data / <i>Date</i>	Pagina / <i>Page</i>
		DT-MATN-2010-04-01	1 Aprile 2010	30 di 30

at the end of the magnetic and gradient longitudinal profile. One possibility is to bent by 90° these terminals to have the necessary coil to coil connections the more possible away from the beam axes and to reduce this undesired effect. Also this detail should be carefully studied if this design will become consistent.

8.4 Pole chamfer optimization

The 12-pole harmonic is generally the most dominant one in this kind of quadrupoles.

To cure this harmonic the pole edge has to be cut with an appropriate chamfer. According to the requirements listed in table I, a chamfer of $2*2$ mm should be enough to vanish the 12-pole harmonic. Obviously this should be checked by simulations and finally determined experimentally.

9. Conclusions

The twin quadrupoles for the Super B Interaction Region, according to table I, can be built using the standard electro-magnetic technology. The computerized calculations are not easy due the particular geometry and shape of the mechanics. Even the coil shape is not standard. It looks like a septum coil with a brazed AISI 316L cooling duct.

However the construction is not so much complicated with the exception of the realization of the copper bar cooling system. If this solution seems to be realistic, the construction of a prototype is strongly suggested, not only to verify the engineering design but also to allow a complete set of magnetic measurements and a complete characterization. So doing, even weak points, if any, can be discovered and, if possible, cured.